

Altered corpus callosum morphology associated with autism over the first 2 years of life

Jason J. Wolff,¹ Guido Gerig,² John D. Lewis,³ Takahiro Soda,^{4,5} Martin A. Styner,^{5,6} Clement Vachet,² Kelly N. Botteron,⁷ Jed T. Elison,⁸ Stephen R. Dager,⁹ Annette M. Estes,¹⁰ Heather C. Hazlett,^{5,6} Robert T. Schultz,¹¹ Lonnie Zwaigenbaum¹² and Joseph Piven^{5,6} for the IBIS Network[†]

[†]For details of the IBIS Network see Appendix 1

Numerous brain imaging studies indicate that the corpus callosum is smaller in older children and adults with autism spectrum disorder. However, there are no published studies examining the morphological development of this connective pathway in infants at-risk for the disorder. Magnetic resonance imaging data were collected from 270 infants at high familial risk for autism spectrum disorder and 108 low-risk controls at 6, 12 and 24 months of age, with 83% of infants contributing two or more data points. Fifty-seven children met criteria for ASD based on clinical-best estimate diagnosis at age 2 years. Corpora callosa were measured for area, length and thickness by automated segmentation. We found significantly increased corpus callosum area and thickness in children with autism spectrum disorder starting at 6 months of age. These differences were particularly robust in the anterior corpus callosum at the 6 and 12 month time points. Regression analysis indicated that radial diffusivity in this region, measured by diffusion tensor imaging, inversely predicted thickness. Measures of area and thickness in the first year of life were correlated with repetitive behaviours at age 2 years. In contrast to work from older children and adults, our findings suggest that the corpus callosum may be larger in infants who go on to develop autism spectrum disorder. This result was apparent with or without adjustment for total brain volume. Although we did not see a significant interaction between group and age, cross-sectional data indicated that area and thickness differences diminish by age 2 years. Regression data incorporating diffusion tensor imaging suggest that microstructural properties of callosal white matter, which includes myelination and axon composition, may explain group differences in morphology.

- 1 Department of Educational Psychology, University of Minnesota, Minneapolis, MN, USA
- 2 Scientific Computing and Imaging Institute, University of Utah, Salt Lake City, UT, USA
- 3 Montreal Neurological Institute, McGill University, Montreal, QC, Canada
- 4 Health Sciences and Technology, Harvard Medical School and Massachusetts Institute of Technology, Boston, MA, USA
- 5 Department of Psychiatry, University of North Carolina at Chapel Hill, Chapel Hill, NC, USA
- 6 Carolina Institute for Developmental Disabilities, University of North Carolina at Chapel Hill, Chapel Hill, NC, USA
- 7 Department of Psychiatry, Washington University at St. Louis, St. Louis, MO, USA
- 8 Institute for Child Development, University of Minnesota, Minneapolis, MN, USA
- 9 Department of Radiology, University of Washington, Seattle, WA, USA
- 10 Department of Speech and Hearing Science, University of Washington, Seattle, WA, USA
- 11 Centre for Autism Research, Children's Hospital of Philadelphia, Philadelphia, PA, USA
- 12 Department of Paediatrics, University of Alberta, Edmonton AB, Canada

Received December 19, 2014. Revised February 24, 2015. Accepted March 6, 2015.

© The Author (2015). Published by Oxford University Press on behalf of the Guarantors of Brain. All rights reserved.

For Permissions, please email: journals.permissions@oup.com

Correspondence to: Jason Wolff, Ph.D.,
Department of Educational Psychology
University of Minnesota
56 East River Road
Minneapolis, MN 55455, USA
E-mail: jjwolff@umn.edu

Keywords: autism; brain development; corpus callosum; infants

Abbreviations: ADOS = Autism Diagnostic Observation Schedule; ASD = autism spectrum disorder; DTI = diffusion tensor imaging

Introduction

Autism spectrum disorder (ASD) emerges early in life, unfolding during a time of dynamic brain and behavioural development. Though severity varies greatly across affected individuals, ASD is characterized by core symptoms of impaired social communication and restricted and repetitive behaviours, as well as associated features including intellectual disability and impaired sensorimotor function. Although less established than many of the behavioural markers associated with the disorder, there has been remarkable progress made toward identifying replicable neural features of ASD. Prominent findings include evidence of cerebral enlargement, evident particularly in early childhood (Piven *et al.*, 1995; Sparks *et al.*, 2002; Redcay and Courchesne, 2005; Schumann *et al.*, 2010; Hazlett *et al.*, 2011; Shen *et al.*, 2013; Zielinski *et al.*, 2014), as well as dynamic, age-dependent patterns of atypical structural and functional connectivity (Just *et al.*, 2007; Wolff *et al.*, 2012; Khan *et al.*, 2013; Nair *et al.*, 2013; Lewis *et al.*, 2014). Identifying the neural markers of ASD specific to infancy, before the consolidation of core behavioural symptoms, may elucidate pathogenesis and provide novel targets for screening and intervention.

Among the most replicated brain imaging findings in ASD is that of a disproportionately small corpus callosum relative to overall brain size. Early MRI studies of autism found significant reductions in the corpus callosum, particularly among posterior regions, in children and adults with autistic disorder relative to control subjects (Egaas *et al.*, 1995; Piven *et al.*, 1997; Manes *et al.*, 1999). More recent work using higher resolution imaging protocols have identified similar reductions in corpus callosum size in adults (Freitag *et al.*, 2009) and both children and adults (Waiter *et al.*, 2005; Just *et al.*, 2007; Hardan *et al.*, 2009; Keary *et al.*, 2009) with ASD. A meta-analysis of this work indicates that decreased corpus callosum size associated with ASD is observed in terms of total corpus callosum area as well as most subdivisions (Frazier and Hardan, 2009). In addition to area and volume, differences have also been observed in corpus callosum thickness, with the splenium and genu particularly 'thinner' in school-age children with the disorder (Vidal *et al.*, 2006). Others have found an inverse relationship between corpus callosum

size and symptom severity in addition to reduced corpus callosum area in school-age children (Hardan *et al.*, 2009) and children and adults with ASD (Prigge *et al.*, 2013). A notable exception to this body of work comes from Lefebvre *et al.* (2015), who found no evidence for corpus callosum differences in a large sample of 7 to 40 year olds with ASD obtained from the ABIDE database of multicentre imaging data. While a notable null finding, that study included only high-functioning individuals whose Autism Diagnostic Observation Schedule (ADOS) severity was at the threshold for ASD cut-off, and did not examine age effects beyond its inclusion as a covariate.

Despite a wealth of cross-sectional data on the corpus callosum in older children and adults with ASD, very little is known about the early development of this structure. The closest exception comes from a study of 4-year-olds indicating decreased total corpus callosum area in children with ASD relative to typically developing peers (Boger-Megiddo *et al.*, 2006). This finding, which was evident only with adjustment for brain volume, extended to five of seven corpus callosum subdivisions. A longitudinal study of corpus callosum morphology in ASD by Frazier *et al.* (2012) identified relatively stable trajectories of decreased corpus callosum volume from ages 8 to 16 years in males with ASD relative to control subjects. Together, these studies provide evidence that atypical corpus callosum morphology may be present from preschool age in ASD, and that the phenomenon is relatively fixed thereafter.

The past two decades of published literature includes over a dozen independent studies identifying a relatively smaller corpus callosum in children and adults with ASD. It is yet unknown whether this morphological difference is evident over the first years of life, during which time the core symptoms of autism first emerge. It is also unknown the extent to which corpus callosum differences extend to unaffected family members who may share features of genetic risk. Neural markers of ASD that emerge early and persist across development may represent promising endophenotypes (Gottesman and Gould, 2003; Iacono and Malone, 2011). Family designs comparing probands with unaffected siblings and control participants are uniquely suited to identify heritable features of psychiatric disorders such as ASD. In this study, we aimed to characterize

developmental trajectories of corpus callosum morphology from ages 6 to 24 months in a prospective sample of infants at low and high familial risk for ASD. We were specifically interested in determining: (i) if and when corpus callosum size in infants with ASD diverged from a typical pattern of development; (ii) whether features of corpus callosum morphology are unique to ASD or shared among high-risk infants; and (iii) whether and how early morphological differences related to later behavioural features. As an ancillary aim, we leveraged diffusion tensor imaging (DTI) data to investigate microstructural properties contributing to observed differences in morphology.

Materials and methods

Participants

Participants were part of the Infant Brain Imaging Study, an ongoing longitudinal study of infants at low- and high-familial risk for ASD. Infants were recruited, screened, and assessed at one of four sites: University of North Carolina, University of Washington, Children's Hospital of Philadelphia, and Washington University in St. Louis. Initial exclusion criteria included: (i) evidence of a genetic condition or syndrome; (ii) significant medical condition affecting development; (iii) significant vision or hearing impairment; (iv) children with birth weight <2000 g or gestational age <36 weeks; (v) significant perinatal adversity or pre-natal exposure to neurotoxins; (vi) contraindication for MRI; (vii) predominant home language other than English; (viii) children who were adopted or half siblings; (ix) first degree relative with psychosis, schizophrenia, or bipolar disorder; and (x) twins.

Infants at high familial risk were defined as such if they had an older sibling with a community diagnosis of ASD, confirmed by the SCQ (Social Communication Questionnaire; Rutter *et al.*, 2003) and Autism Diagnostic Interview-Revised (Lord *et al.*, 1994). Infants at low familial risk were defined by virtue of having a typically developing older sibling who screened negative on the SCQ and no first degree relatives with a developmental disability. All study procedures were approved by institutional review at each site, and informed, written consent was obtained from all participants.

This study included children with imaging data for at least one time point and a complete diagnostic assessment at age 2 years. Participants were grouped by familial risk status (low- or high-risk sibling) and diagnostic outcome based on clinical best estimate made by experienced, licensed clinicians using the DSM-IV-TR (Diagnostic and Statistical Manual of Mental Disorders, 4th Edition, Text Revision) checklist and supported by all available behavioural assessment data. Diagnostic classification for each case was independently verified based on video and record review by a second clinician naïve to risk and initial classification. Three low-risk children meeting criteria for ASD were excluded as this group was too small to analyse separately. One child from the low-risk control group was excluded for evidence of severe/profound global developmental delay. This approach to group classification yielded 378 total participants: 108 low-risk controls without ASD, 213 children classified as high-risk ASD negative, and 57

children classified as high-risk ASD-positive. Children meeting criteria for ASD or autism on the ADOS but who were determined by clinicians not to have the disorder were included in the high-risk ASD-negative group to maintain naturally occurring heterogeneity. The majority of participants (83%) contributed imaging data for two or more time points. There were no group differences in proportion of scan failures between risk or diagnostic groups. Descriptive and demographic data for study participants are presented in Table 1.

Clinical measures

The ADOS (Lord *et al.*, 2000) is a semi-structured assessment of behavioural symptoms associated with ASD. It provided information contributing to clinical best estimate determination as well as an overall severity score (Gotham *et al.*, 2009), a standardized measure reflecting social affect and repetitive behaviour symptoms observed during administration of the ADOS. The ADOS also yields domain scores for Social Affect and Restricted and Repetitive Behaviours, the former of which was used to characterize the relationship of morphological features to social-communicative symptoms associated with ASD. The Repetitive Behaviour Scales-Revised (RBS-R; Bodfish *et al.*, 2000) is a parent rated measure of severity and repertoire of repetitive behaviour. RBS-R 'total repetitive behaviours endorsed' shows good dimensionality at age 2 and was selected over the ADOS to characterize this symptom domain in relation to imaging measures (Wolff *et al.*, 2014). The Mullen Scales of Early Learning (Mullen, 1995) is a standardized developmental assessment for children from birth to 68 months. The Mullen provides an Early Learning Composite score, which reflects overall cognitive and motor skill development. Mullen scores from age 12 months were used for two participants missing complete data at 24 months. Clinical assessment reliability was established and maintained through monthly cross-site calibration.

Image acquisition

MRI scans were acquired on identical 3 T Siemens TIM Trio scanners equipped with 12-channel head coils during natural sleep. The imaging protocol included: sagittal T₁ MPRAGE (repetition time = 2400 ms, echo time = 3.16 ms, slice thickness = 1 mm, field of view = 256 mm, 256 × 160 matrix), 3D T₂ fast spin echo (repetition time = 3200 ms, echo time = 499 ms, slice thickness = 1 mm, field of view = 256 mm, 256 × 160 matrix), and 25-direction ep2d_diff sequence with field of view = 190 mm (6 and 12 months) or field of view = 209 mm (24 months), 75–81 transversal slices, slice thickness = 2 mm isotropic, 2 × 2 × 2 mm³ voxel resolution, repetition time = 12 800–13 300 ms, echo time = 102 ms, variable b-values between 0 and 1000 s/mm². Intra- and inter-site reliability was initially established and maintained across clinical sites over time through traveling human phantoms (Gouttard *et al.*, 2008).

Corpus callosum segmentation

Initial preprocessing of T₁-weighted images provided a rigid alignment to normative atlas space where the cross-section of the corpus callosum was aligned with the midsagittal plane.

Table 1 Descriptive and demographic data

	High-risk ASD-positive	High-risk ASD-negative	Low-risk-Neg	P ^a
Total participants	57	213	108	
6 m scan	9	14	8	
12 m scan	1	18	7	
24 m scan	6	8	4	
6 and 12 m scans	2	32	33	
6 and 24 m scans	5	15	11	
12 and 24 m scans	10	42	8	
6, 12 and 24 m scans	24	84	37	
Age (Time 1)	6.6 (0.7)	6.6 (0.7)	6.7 (0.7)	0.78
Age (Time 2)	12.9 (0.8)	12.6 (0.6)	12.7 (0.7)	0.13
Age (Time 3)	24.8 (1.2)	24.8 (1.0)	24.7 (0.8)	0.92
ADOS severity^b	5.8 (1.8)	1.6 (1.1)	1.5 (0.9)	<0.001
IQ^c	79.8 (17.6)	101.7 (15.9)	110.9 (16.0)	<0.001
Sex (% male)^d	82.5	57.3	61.1	0.001
Mother's education^e (% college or higher)	59.6	68.5	83.3	0.002

^aOmnibus ANOVA (Age, ADOS severity, IQ) and Fisher's exact tests (mother's education, sex).

^bAvailable for 99% of total sample. Pairwise: high-risk ASD-positive > high-risk ASD-negative, low-risk ASD-negative.

^cMullen Early Learning Composite. Pairwise: low-risk ASD-negative > high-risk ASD-negative > high-risk ASD-positive.

^dProportion of males: high-risk ASD-positive > high-risk ASD-negative, low-risk-negative.

^eProportion of mothers with college degree or higher: low-risk ASD-negative > high-risk ASD-negative, high-risk ASD-positive.

Sagittal slices within ± 2 mm of the midsagittal plane (five total slices) were averaged to create the single 2D image within which the corpus callosum was segmented. Segmentation was performed via the CCseg tool (Vachet *et al.*, 2012) which uses a statistical model of contour shape and image appearance of the corpus callosum (Székely *et al.*, 1996; Vachet *et al.*, 2012) based on the concept of active appearance models (Cootes *et al.*, 2001). Starting from the average shape, the corpus callosum contour is iteratively deformed to match the image intensities while restricting deformations to the model shape statistics. In a final step, the contour is deformed without restrictions but only within a close neighbourhood. The model used here was trained with image data from an independent paediatric study (Cascio *et al.*, 2006). Through the model deformation, this approach provides a direct point-to-point correspondence of corpus callosum boundaries for all subject images. Contours were visually inspected by a blind rater (T.S.) for quality of segmentation and manually corrected through re-initialization or insertion of a repulsion point to restrain the model (Vachet *et al.*, 2012). Approximately 12% of cases required manual correction based on visual quality control. About 5% of image data required simple re-initialization (i.e. the initial translation and rotation that aligns the average corpus callosum contour to the image prior to deformation), while for 7% manual expert refinement of contour segmentation was applied by adding a repulsion point (Kass, 1988) to allow the contour to find a state of minimum energy. Within- and between-rater reliability for manual refinement of corpus callosum contours has been previously reported for this sample as 0.99 (Vachet *et al.*, 2012). There were no significant differences among groups for proportion of data requiring manual correction.

Brain volume segmentation

Brain tissue volumes were obtained through a framework of atlas-moderated expectation-maximization with co-registration

of T₁- and T₂-weighted MRI images, bias correction, skull stripping, and multimodal tissue classification using the AutoSeg toolkit (<http://www.nitrc.org/projects/autoseg/>). Population average templates and corresponding probabilistic brain tissue priors for grey and white matter were created for the 6, 12, and 24 month old brain. Grey and white matter volumes were summed to yield an estimate of total brain volume.

Medial axis representation

Variability in corpus callosum shape is subject to extrinsic factors such as rotation or bending, resulting from variance in brain shapes or type of image alignment, as well as intrinsic shape properties as measured by object length and local thickness, i.e. measurements that are invariant to the anatomical coordinate system. Whereas traditional methods of corpus callosum shape measurement are subject to both sources of variance, our analysis focused on intrinsic shape properties. We followed the framework of medial axis transformation, which results in a representation that is invariant to rotation, translation and bending (Styner *et al.*, 2003). Following Sun *et al.* (2007), the corpus callosum contour parameterization is transformed into a process-induced symmetric axis where corpus callosum shapes are represented by the medial axis between the end points of genu and splenium (length), with local width (or thickness) attributed to each medial axis point. Starting from 100 equidistant contour points and after resampling of the medial axis into equidistant length intervals, we computed 25 medial axis points with attributed local thickness. It is important to note that our segmentation results in parametric representations of corpus callosum boundaries which after conversion to invariant shapes leads to one-to-one point correspondences across subjects and age groups (Székely *et al.*, 1996). Supplementary Fig. 1 illustrates corpus callosum boundaries, medial axis definition and location, and thickness measurements across age intervals.

DTI data processing

Diffusion-weighted images were first processed with DTIPrep to automatically detect common artefacts, correct for motion and eddy current deformations, and exclude bad gradients (Liu *et al.*, 2010; Oguz *et al.*, 2014). Following this step, expert raters manually removed gradients presenting residual artefacts. Data sets with fewer than 18 remaining gradients were excluded from further processing to ensure consistent signal-to-noise ratio. Post-processing analysis found no significant differences between diagnostic outcome groups in terms of motion or other artefacts affecting image quality. Group analysis of diffusion weighted data used a previously reported pipeline which provides consistent spatial parameterization within and between individual data sets across age groups in a common atlas space (Goodlett *et al.*, 2009; Verde *et al.*, 2014).

Corpus callosum tractography was accomplished through seed label mapping of the midsagittal atlas image using 3D Slicer (www.slicer.org), with acquired data limited to the three centremost slices. Label maps for three subdivisions of the corpus callosum were created based on segmentations described by Witelson (1989). Resulting fibre track definitions were processed for spurious or incomplete streamlines using 3D Slicer and FibreViewerLight prior to fibre parameterization and generation of fibre track data using DTIAtlas FibreAnalyzer (Verde *et al.*, 2014). The open-source tools constituting this DTI processing pipeline are publically available through the UNC-Utah NA-MIC DTI fibre tract analysis framework (www.nitrc.org/projects/namicdtifibre).

Statistical analysis

Longitudinal trajectories of corpus callosum morphology across 6, 12 and 24 months of age were analysed using repeated measures mixed models with unstructured covariance matrices. This analytic approach allows for different patterns of missing data and accommodates an unbalanced design. Our primary set of dependent variables included total area, mean thickness, and mean length. Independent variables of interest included group, age, and the group \times age interaction. A quadratic age term (age^2) was added to the model for length based on *a priori* visual analysis of graphed data. Total brain volume was included as a covariate given its known relationship to corpus callosum size as well as published data suggesting increased brain volume among young children with ASD (Hazlett *et al.*, 2011; Shen *et al.*, 2013). Other control variables included site, to account for possible variance related to scan sites, as well as factors which differed significantly between groups: sex, Mullen Early Learning Composite, and mother's education (Table 1). Potential effects of an age \times site interaction were vetted and ultimately excluded from the primary analysis (Supplementary material). To elucidate the effect of total brain volume on primary model results, follow-up analyses omitting this factor were also generated.

Estimated marginal means for each imaging time point (6, 12 and 24 months) were generated from our primary model described above and tested for cross-sectional group differences. Following significant omnibus results, Bonferroni corrected pairwise comparisons were performed and estimates of effect size generated based on estimated marginal means and

standard errors. In a separate set of analyses, correlations controlling for total brain volume were generated to investigate whether corpus callosum morphology (6 and 12 months) was associated with later clinical outcomes measured at age 24 months. Clinical variables of interest included Mullen Early Learning Composite scores, ADOS social affect scores, and total inventory of repetitive behaviour from the RBS-R. These latter two measures were selected to disaggregate social affect and repetitive behaviour symptom domains. All tests excepting *post hoc* comparisons were two-tailed with $\alpha = 0.05$.

Results

Demographic and clinical characteristics for participants are presented in Table 1. Groups did not differ by age at any of the three time points. Omnibus results indicated that autism symptom severity based on the ADOS at age 2 differed significantly among groups, $F(2,372) = 313.9$, $P < 0.001$. Consistent with classification according to clinical outcome, autism severity was significantly higher among children classified as high-risk ASD-positive relative to either high-risk or low-risk ASD-negative groups ($P < 0.001$), but did not differ between children classified as high-risk ASD-negative and low-risk ASD-negative ($P = 0.61$). There were significant group differences with respect to sex (Fisher's exact test, $P = 0.001$) and Mullen Early Learning Composite score, $F(2,375) = 69.4$, $P < 0.000$ (Table 1). Groups also differed in terms of mother's education (Fisher's exact test, $P = 0.002$), with low-risk controls having a higher proportion of mothers with a college degree or greater.

Longitudinal and cross-sectional comparisons of corpus callosum morphology

Our primary set of analyses compared trajectories of midsagittal corpus callosum total area, length, and thickness between outcome groups over the 6- to 24-month age interval with adjustment for total brain volume, sex, mother's education, site, and Mullen Early Learning Composite. For total area, there was a significant effect for group, $F = 3.4$, $P = 0.036$ and age, $F = 538.7$, $P < 0.001$, but not group \times age, $F = 0.22$, $P = 0.80$. *Post hoc* comparisons for total area \times group did not survive correction for multiple comparisons.

We next proceeded to the primary components constituting area: length and thickness. For length, there was a significant effect for age² ($F = 8.5$, $P = 0.004$) but not group ($F = 0.4$, $P = 0.69$) or the group \times age² interaction ($F = 0.5$, $P = 0.64$). For thickness, there was a significant effect for group ($F = 6.1$, $P = 0.002$) and age ($F = 514.6$, $P < 0.001$) but not the group \times age interaction ($F = 0.42$, $P = 0.66$). Mixed-model adjusted trajectories for corpus callosum total area, length, and thickness are presented in Fig. 1.

Post hoc results indicated that thickness was significantly greater for high-risk ASD-positive children relative to low-risk ASD-negative ($P = 0.008$, $d = 0.57$) and near the threshold for significance relative to high-risk ASD-negative ($P = 0.07$, $d = 0.40$). High-risk- and low-risk ASD-negative groups did not significantly differ from one another ($P = 0.29$, $d = 0.20$).

Primary model results, as well as secondary analyses omitting adjustment for total brain volume, are presented in Table 2. Cross-sectional comparisons based on model data made at each imaging time point (6, 12, and 24 months) indicated that the group effect for thickness was strongest at age 6 months and statistically non-significant by age 24 months (Table 3).

Localization of thickness differences

The main set of analyses pinpointed thickness as the primary driver of group differences in midsagittal corpus callosum shape. To characterize this phenomenon in greater detail, we generated effect size estimates (Cohen's d) based on primary model adjusted data for 25 regions comprising the totality of the corpus callosum (Fig. 2). Cross-sectional pair-wise comparisons for these regions did not survive false-discovery rate correction. Per cent difference in model-adjusted thickness values were also generated (Supplementary Fig. 2). Pairwise differences were particularly robust between high-risk ASD-positive and low-risk ASD-negative groups at ages 6 and 12 months (Fig. 2). At age 6 months, the strongest of these effects corresponded to regions implicated in prefrontal, pre-/supplementary motor, and posterior-parietal connectivity (Hofer and Frahm, 2006). At age 12 months, an increased effect was seen in regions corresponding with primary motor connectivity, while posterior differences became less robust. By age 24 months, effect sizes were weak overall, with posterior regions showing an inverse pattern relative to that observed at age 6 months.

Contribution of microstructural properties to thickness

Thickness results indicated that the anterior portion of the corpus callosum was particularly enlarged in ASD from ages 6 to 12 months. Based on previous work, we hypothesized that corpus callosum overgrowth for this region in human infants could stem from an excess of thin axons secondary to excessive axon branching or deficient pruning (Cowan et al., 1984; LaMantia and Rakic, 1990; Aboitiz et al., 1992) as well as differences in myelination. To address this hypothesis, we examined the contribution of radial diffusivity in the centremost three slices of the anterior third of the corpus callosum to thickness in this region. We centred this analysis at the approximate midpoint of 12 months of age, which also represented the time point with the largest number of subject scans. Radial diffusivity reflects diffusion orthogonal to the primary axis of the fibre bundle. While not a direct measure of axon composition or density, radial diffusivity was selected over alternative measures (e.g. axial or mean diffusivity) given its higher sensitivity to these factors (Klawiter et al., 2011). The anterior corpus callosum was selected given both its relevance in the current findings as well as previous work suggesting that size in this region is particularly linked to axon composition (Aboitiz et al., 1992; Hofer and Frahm, 2006).

A three-step hierarchical multiple regression analysis was performed with mean thickness of the anterior third of the corpus callosum fit as the dependent variable. Independent variables entered into Step 1 included age, sex, site, total brain volume, and Mullen Early Learning Composite. Step 2 added radial diffusivity for the anterior third of the corpus callosum. Collinearity diagnostics indicated good model stability (all VIF < 1.4, tolerance > 0.7). Variables included in Step 1 accounted for $R^2 = 0.04$ and differed significantly from zero, $F(5,258) = 2.3$, $P = 0.046$. In Step 2, radial diffusivity of the anterior third of the corpus callosum was added as an independent variable. The addition of this variable resulted in a significant change in R^2 ,

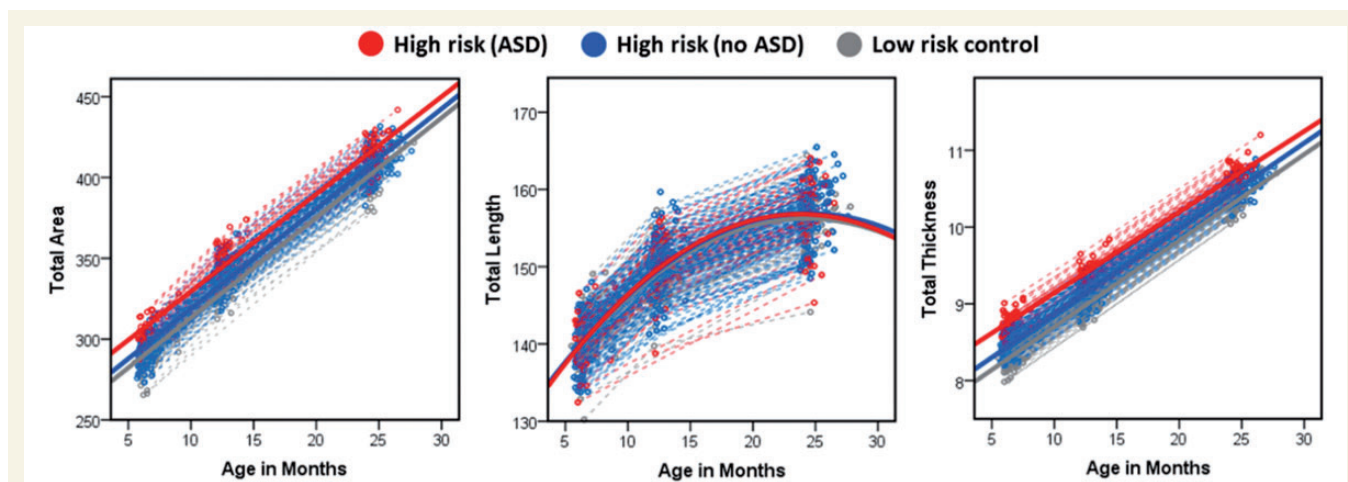


Figure 1 Mixed model adjusted trajectories for corpus callosum morphological features across risk-by-diagnosis groups.

$F(1,258) = 209.8$, $P < 0.001$. The full model for Step 2 was significantly greater than zero, $F(6,258) = 38.5$, $P < 0.001$, $R = 0.69$, $R^2 = 0.48$. Radial diffusivity in the anterior portion of the corpus callosum significantly predicted thickness of this region, standardized $\beta = -0.69$, $P < 0.001$. A scatterplot of unadjusted radial diffusivity and corpus callosum thickness values is presented in Fig. 3. As an exploratory Step 3, we examined the addition of the interaction of group \times radial diffusivity. The addition of this term resulted in a significant change in R^2 , $F(1,258) = 10.1$, $P = 0.002$, and a model which differed significantly from zero, $F(6,258) = 35.6$, $P < 0.001$, $R = 0.71$, $R^2 = 0.50$,

suggesting that diagnostic group status moderates the relationship between radial diffusivity and corpus callosum thickness.

To further vet these results, we conducted two follow-up analyses. First, we examined axial diffusivity (diffusivity along the primary fibre orientation) in relation to anterior corpus callosum thickness. This factor significantly predicted thickness albeit with smaller effect size than for radial diffusivity ($R^2 = 0.15$ for axial diffusivity versus 0.48 for radial diffusivity). Second, we examined the contribution of radial diffusivity to thickness in the splenium, or posterior fifth, of the corpus callosum given its potential role in the early development of ASD (Elison *et al.*, 2013). A regression model including splenium radial diffusivity significantly predicted posterior corpus callosum thickness, $F(6,258) = 11.8$, $P < 0.001$, $R = 0.47$, $R^2 = 0.22$, suggesting a similar albeit attenuated relationship between microstructure and thickness relative to that observed in the anterior corpus callosum. See [Supplementary material](#) for full model results for anterior axial diffusivity and splenium radial diffusivity.

We next expanded upon the results for radial diffusivity in relation to anterior thickness by broadening our analysis to all three time points using repeated measures mixed models. First, we sought to determine whether radial diffusivity was associated with corpus callosum thickness across all three time points by fitting a model with anterior corpus callosum radial diffusivity, age, sex, site, total brain volume, and Mullen Early Learning Composite fit as independent variables and anterior corpus callosum thickness as the dependent variable. There was a significant effect for radial diffusivity in the anterior portion of the corpus callosum over 6, 12, and 24 months, $F = 101.1$, $P < 0.001$, indicating that radial diffusivity is inversely associated with thickness

Table 2 Longitudinal mixed-model results with and without adjustment for total brain size¹

Corpus callosum feature	Adjusted for total brain volume		Unadjusted for total brain volume	
	F	P	F	P
Total area				
Group	3.4	0.04	3.8	0.02
Age	538.7	<0.001	2859.4	<0.001
Group \times Age	0.2	0.80	0.3	0.75
Length				
Group	0.4	0.69	0.3	0.72
Age	8.5	0.004	1214.6	<0.001
Group \times Age	0.5	0.64	0.5	0.95
Thickness				
Group	6.1	0.002	6.0	0.003
Age	514.6	<0.001	1660.6	<0.001
Group \times Age	0.4	0.66	0.4	0.70

¹All models adjusted for sex, site, mother's education, and Mullen Early Learning Composite.

Table 3 Cross-sectional estimated marginal means by group for midsagittal corpus callosum shape

Corpus callosum feature	High-risk ASD-positive (A)		High-risk ASD-negative (B)		Low-risk ASD-negative (C)		Omnibus ^a		Post hoc ^b	Cohen's d	
	EMM	SE	EMM	SE	EMM	SE	F	P		(A) vs. (B)	(A) vs. (C)
Time 1 (6 months)											
Total area	307.44	6.97	299.56	3.28	293.69	4.39	1.4	0.26			
Length	139.03	1.85	141.58	0.87	141.95	1.17	0.9	0.41			
Thickness	8.92	0.15	8.56	0.07	8.35	0.10	4.7	0.01	a > b,c	0.42	0.61
Time 2 (12 months)											
Total area	346.52	8.00	339.80	3.27	329.04	4.95	2.2	0.12			
Length	148.71	1.81	150.58	0.74	149.69	1.12	0.6	0.54			
Thickness	9.38	0.17	9.12	0.07	8.86	0.10	3.5	0.03	a > c, b > c	0.28	0.55
Time 3 (24 months)											
Total area	402.48	8.41	405.16	4.18	408.50	6.61	0.2	0.85			
Length	155.06	1.73	156.68	0.86	158.74	1.36	1.4	0.25			
Thickness	10.44	0.18	10.44	0.09	10.35	0.14	0.2	0.87			

^aMixed effects model. Two-sided significance level of 0.05.

^bBonferroni corrected.

EMM = estimated marginal mean; SE = standard error.

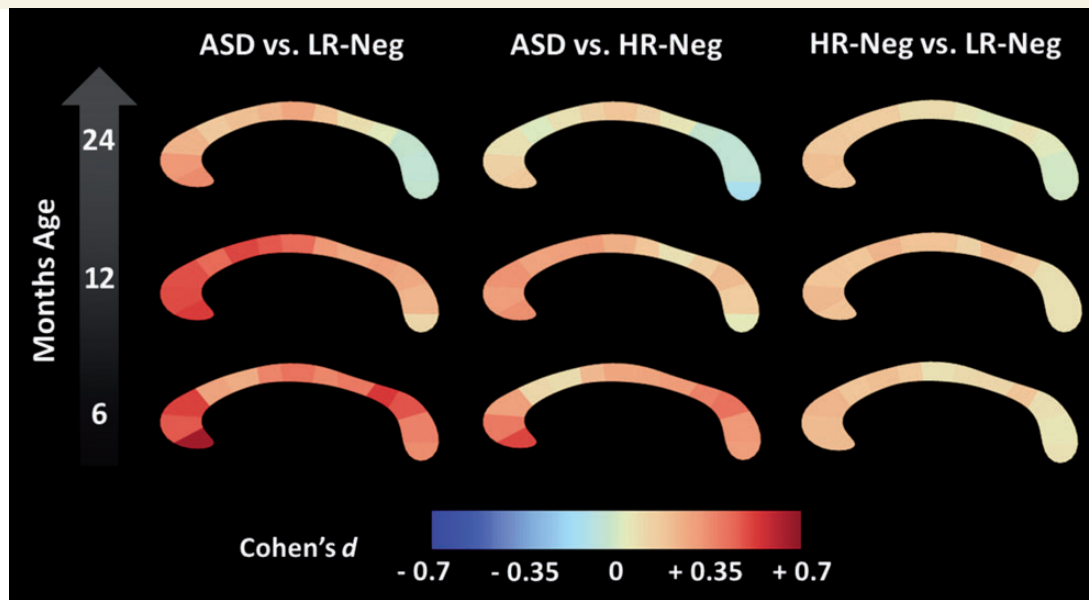


Figure 2 Longitudinal effect size. Longitudinal effect size data (Cohen's d) for pairwise corpus callosum thickness differences among high-risk infants who developed autism spectrum disorder (ASD), high-risk infants without ASD (HR-Neg), and low-risk controls (LR-Neg).

across these ages. Second, we fit a model with radial diffusivity as the dependent variable, and age, sex, site, and Mullen Early Learning Composite as independent variables. Total brain volume was omitted from this model as local diffusion properties should not theoretically vary as a function of brain size. We identified a significant effect for group ($F = 3.5$, $P = 0.03$) characterized by higher radial diffusivity among children with ASD, with group \times time near the critical value, $F = 2.9$, $P = 0.059$ (Fig. 4). While appearing initially counter to the inverse relationship between radial diffusivity and thickness, the pattern seen in Fig. 4 is consistent with Step 3 of our regression model, wherein diagnostic group status exerts a significant moderating effect on the relationship between radial diffusivity and corpus callosum thickness.

Relationship of corpus callosum thickness to behavioural outcomes

Correlations controlling for total brain volume were generated for primary corpus callosum measures at ages 6 and 12 months, as well as change rate across this interval, with select clinical outcome measures at age 24 months among children with ASD. Mullen Early Learning Composite and ADOS Social Affect domain scores at age 24 months were not significantly correlated with 6 or 12 month measures of total corpus callosum area, length, or thickness. Total repetitive behaviour endorsed on the RBS-R at age 24 months was significantly correlated with both corpus callosum area ($r = 0.52$, $P = 0.005$) and thickness ($r = 0.50$, $P = 0.007$), but not length ($r = 0.29$, $P = 0.14$), at the 6-month time point. Repetitive behaviour endorsed was

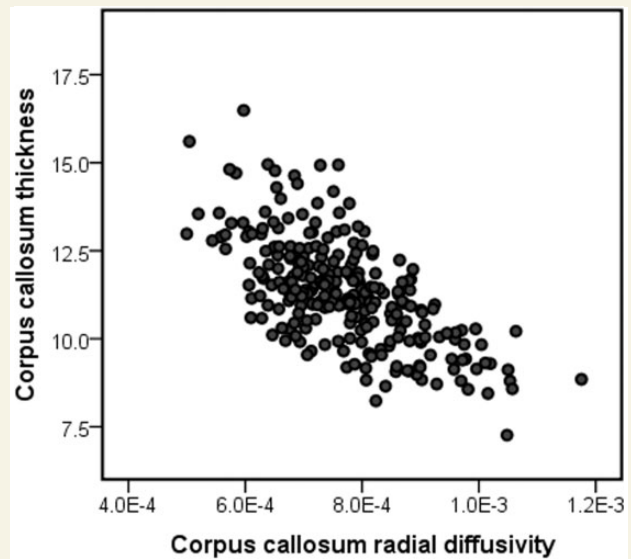
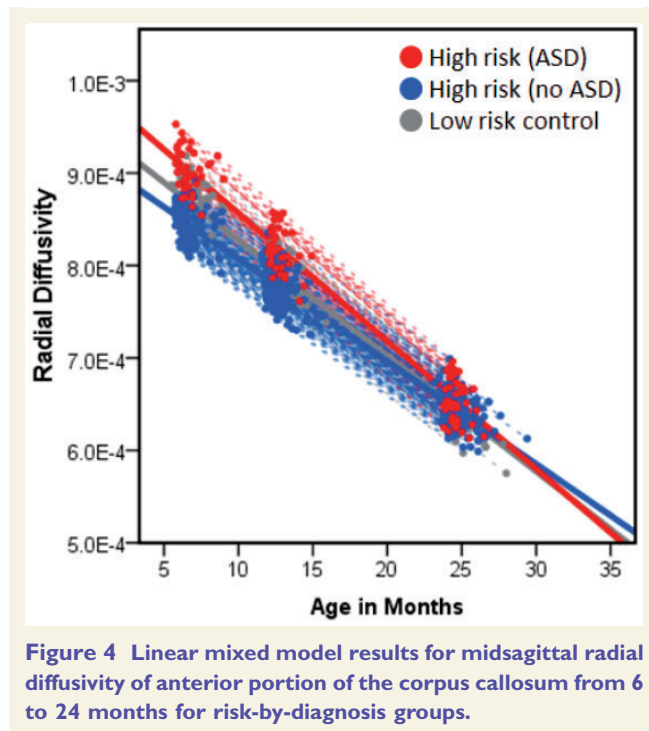


Figure 3 Unadjusted scatterplot of midsagittal radial diffusivity values in relation to thickness for the anterior third of the corpus callosum for total study sample centred at age 12 months.

significantly correlated with thickness ($r = 0.44$, $P = 0.03$), but not area or length, at age 12 months. For children with data at both 6 and 12 months of age, monthly change rate was not significantly associated with behavioural measures.

Discussion

The corpus callosum is a prominent and highly-organized white matter structure comprised of long-range nerve fibres



providing functional coordination between homologous brain regions. Though implicated by studies of older children and adults with ASD, little is known about its role in the early emergence of the disorder. In this prospective, longitudinal study, we found significantly increased midsagittal corpus callosum area in infants who later developed ASD. These differences were driven by in-plane thickness rather than length, with thickness of the anterior corpus callosum particularly greater in babies who developed ASD relative to comparison children who did not (Fig. 2). Differences in corpus callosum size appeared strongest at age 6 months, with the effect diminishing by age 2 years (Fig. 2). Unaffected high-risk siblings differed from controls in corpus callosum thickness at age 12 months only, suggesting either the presence of a subpopulation who may later meet criteria for a neurodevelopmental disorder or the low-level expression of a shared but developmentally variant phenotypic feature. The presence of disease-specific morphological differences at 6-months of age is of particular significance and suggests that corpus callosum overgrowth could be among the earliest neural signatures of autism.

It is noteworthy that the present results are in distinct contrast to findings of a disproportionately smaller corpus callosum among older individuals with ASD (Frazier *et al.*, 2012). While not consistent among studies (Lefebvre *et al.*, 2015), smaller corpus callosum size has been observed even among preschool aged children who are but a few years older than those in our sample (Boger-Megiddo *et al.*, 2006). That we found increased corpus callosum size in ASD, regardless of adjustment for total brain volume, suggests the interplay of neurodevelopmental processes unique

to infancy. At the macro level, this includes the rapid growth of callosal white matter and cerebral cortex over the first year of life, after which time development of these regions gradually wanes (Deoni *et al.*, 2012; Gilmore *et al.*, 2012; Sadeghi *et al.*, 2013). These early changes, observed through MRI, stem from micro-level events including progenitor cell proliferation and differentiation, apoptosis, process elimination, as well as arborization, myelination, and axon growth (Low and Cheng, 2006). Disruption to one or more of these developmental events during infancy—which occur in advance of the clinical presentation of autism—may set the stage for the later-emerging patterns of callosal undergrowth. Considered within a developmental framework, morphological findings which initially appear incongruent may in fact reflect early versus later neural features of ASD (Uddin *et al.*, 2013).

Given the robust nature of axonal pruning known to occur in the corpus callosum early in life (Cowan *et al.*, 1984; LaMantia and Rakic, 1990), we hypothesized, based on the correspondence of timing to this unique developmental event (Workman *et al.*, 2013), that overgrowth in infants who developed ASD may reflect an excess of thin axons secondary to axon over-production or dampened developmental elimination. As an initial test of this hypothesis, we explored the relationship between callosal microstructure, measured using DTI, and callosal morphology. We found a significant inverse relationship between local radial diffusivity and anterior callosal thickness, with a full model including covariates accounting for nearly 50% of variance. This suggests that corpus callosum size in early childhood varies as a function of microstructure possibly linked to axon composition, an interpretation in-line with post-mortem (Aboitiz *et al.*, 1992) and other DTI findings (Hofer and Frahm, 2006; Klawiter *et al.*, 2011). We further identified an interaction between diagnostic status and radial diffusivity on corpus callosum thickness, suggesting that an as yet unknown mechanism may moderate the nature of the relationship between radial diffusivity and corpus callosum growth among babies who later develop ASD.

While early increases in corpus callosum size may stem from an overabundance of thin axons, increased myelination, or both, inadequate experience-dependent axon growth and refinement may explain later findings of corpus callosum undergrowth associated with ASD (Markham *et al.*, 2009; Paus, 2010; Zikopoulos and Barbas, 2010). In typically developing children, rapid corpus callosum growth has been observed through adolescence (Giedd *et al.*, 1999; Lenroot *et al.*, 2007). This growth, which outpaces apoptosis and axon elimination, occurs absent a strong effect for myelin content on maturation for both typically developing children (Perrin *et al.*, 2009; Paus, 2010) and children with ASD (Gozzi *et al.*, 2012). This implicates plasticity involving axonal refinement rather than either aberrant myelination or atypical g ratio (Paus and Toro, 2009). An early overabundance of thin axons, followed by suboptimal refinement and growth,

could plausibly explain the contrast between the present findings and those from older children with ASD. While we did not identify a statistically significant effect for group \times age, group differences in corpus callosum thickness decreased from ages 6 to 24 months (Fig. 2). We anticipate that typically developing children may ‘catch up’ with and surpass children with ASD in terms of corpus callosum size by school age as increased axon calibre and myelin content begins to outpace overgrowth initially associated with thin axon over-abundance (Boger-Megiddo *et al.*, 2006). There is some evidence of this possibility in our data at age 2 years, wherein the posterior corpus callosum appears marginally thinner in children with ASD, consistent with findings from older children (Vidal *et al.*, 2006).

With regard to the relationship between the corpus callosum and clinical features among infants who developed ASD, we found that morphological features at both 6 and 12 months of age positively predicted repetitive behaviours measured at age 2 years. We did not, however, see a relationship between corpus callosum morphology and either IQ or social symptoms despite precedence for this later in life (Hardan *et al.*, 2009; Keary *et al.*, 2009; Prigge *et al.*, 2013). The link between corpus callosum morphology and repetitive behaviour may reflect the scaffolding of neural architecture and behaviour in support of functional specialization involving more complex skills. For example, recent work from our group has implicated posterior corpus callosum microstructure in basic visual orienting function in 7-month-old infants, an early structure–function relationship likely supporting distal social skill development (Elison *et al.*, 2013). The relationship between morphology and repetitive behaviour features of ASD in infants may similarly reflect a fundamental but age-dependent role for the corpus callosum in early sensory-motor development. The robust differences in the anterior corpus callosum lend credence to this interpretation. These regions, which are involved in pre-/supplementary motor and orbitofrontal circuitry, have been implicated in sensory function and behavioural inhibition generally and repetitive behaviours specifically (Giedd *et al.*, 1994; Langen *et al.*, 2011).

Evidence for altered corpus callosum morphology in infants who develop ASD is in keeping with evidence of increased brain volume (Hazlett *et al.*, 2011; Shen *et al.*, 2013) as well as prevailing theory concerning the essential yet indeterminate role of connectivity (Uddin *et al.*, 2013; Lewis *et al.*, 2014). Recent evidence of cortical surface area expansion in the first year of life (Hazlett *et al.*, submitted for publication) and accounts of aberrant neurogenesis and neuronal migration (Casanova *et al.*, 2006; Courchesne *et al.*, 2011) implicate events unique to prenatal and early postnatal development. For infants who develop ASD, these neurodevelopmental events, including postnatal remodelling of the corpus callosum, are co-occurring in an altered context. The aberrant corpus callosum growth observed in the present study, concomitant with brain enlargement, may induce later conduction delays (Lewis and Elman, 2008)

and decreased network efficiency, particularly among long-distance connections such as those supported by corpus callosum fibres (Lewis *et al.*, 2014).

Limitations

Participants in this study were grouped based upon clinical best-estimate diagnosis made at age 2 years. While similar work has found strong diagnostic stability from age 2 (e.g. Shen *et al.*, 2013), it is feasible that some children judged high-risk ASD-negative or high-risk ASD-positive may change diagnostic classification by school-age. Following children past early childhood would offer the opportunity to account for dynamic changes in diagnostic status and more accurately establish patterns of brain–behaviour development. Further, while our DTI data suggest axonal development may explain morphological differences in the corpus callosum, factors such as pruning, myelination, and axon calibre change are not mutually exclusive phenomenon, and each of these processes likely contributes both to morphology and local diffusion values (Mori and Zhang, 2006). This, along with other potential sources of error inherent to DTI, limits the extent to which causal inferences may be made and necessitates corroboration through complimentary imaging measures and non-human animal model work.

Conclusion

Although atypical connectivity associated with autism is not limited to commissural pathways, numerous studies have identified corpus callosum differences among individuals with ASD using functional MRI (Just *et al.*, 2007; Anderson *et al.*, 2011; Schipul *et al.*, 2012), DTI (Alexander *et al.*, 2007; Kumar *et al.*, 2010; Shukla *et al.*, 2010; Lewis *et al.*, 2013), magnetization transfer imaging (Gozzi *et al.*, 2012) and structural MRI (Frazier and Hardan, 2009). Among toddlers with ASD, there is evidence from functional MRI during natural sleep of decreased interhemispheric synchronization associated with symptom severity and language function (Dinstein *et al.*, 2011). Findings from multimodal imaging studies of the corpus callosum have linked structure and function by demonstrating that size is positively correlated with functional synchrony in adolescents and adults with ASD (Just *et al.*, 2007; Schipul *et al.*, 2012) and inversely associated with measures of fibre length, suggesting diminished connectivity (Lewis *et al.*, 2013). On the basis of these published data, we may conclude that corpus callosum connectivity, broadly defined, is implicated in ASD. However, given that much of the published literature involves individuals who already have the disorder, the pathogenic versus collateral role of corpus callosum development in ASD cannot be ascertained. The present work adds a new dimension to existing knowledge by suggesting that the corpus callosum is indeed temporally implicated in

the emergence of ASD, but that the nature of this relationship appears to materially differ from what has been reported later in the course of the disorder.

Acknowledgements

Thanks to J. Ryan Scotton and Rachel Gimpel Smith for their assistance with data processing and quality control. We sincerely thank our IBIS families for participating in this research.

Funding

This study was supported by grants from the National Institute of Child Health and Development (R01-055741, 055741-S1, and P30-03110, U54-079124), Autism Speaks, and the Simons Foundation to J.P.; a grant from the National Institute of Mental Health (K01-101653) to J.J.W., a student fellowship award from the American Academy of Child and Adolescent Psychiatry to T.S., and the National Alliance for Medical Image Computing, funded by the NIH Roadmap for Medical Research (U54-EB005149).

Supplementary material

Supplementary material is available at *Brain* online.

References

- Aboitiz F, Scheibel AB, Fisher RS, Zaidel E. Fiber composition of the human corpus callosum. *Brain Res* 1992; 598: 143–53.
- Alexander AL, Lee JE, Lazar M, Boudos R, DuBray MB, Oakes TR, et al. Diffusion tensor imaging of the corpus callosum in autism. *Neuroimage* 2007; 34: 61–73.
- Anderson JS, Druzgal TJ, Froehlich A, DuBray MB, Lange N, Alexander AL, et al. Decreased interhemispheric functional connectivity in autism. *Cereb Cortex* 2011; 21: 1134–46.
- Bodfish JW, Symons FJ, Parker DE, Lewis MH. Varieties of repetitive behavior in autism: comparisons to mental retardation. *J Autism Dev Disord* 2000; 30: 237–43.
- Boger-Megiddo I, Shaw DWW, Friedman SD, Sparks BF, Artru AA, Giedd JN, et al. Corpus callosum morphometrics in young children with autism spectrum disorder. *J Autism Dev Disord* 2006; 36: 733–9.
- Casanova MF, van Kooten IAJ, Switala AE, van Engeland H, Heinsen H, Steinbusch HWM, et al. Minicolumnar abnormalities in autism. *Acta Neuropathol* 2006; 112: 287–303.
- Cascio C, Styner M, Smith RG, Poe MD, Gerig G, Hazlett HC, et al. Reduced relationship to cortical white matter volume revealed by tractography-based segmentation of the corpus callosum in young children with developmental delay. *Am J Psychiatry* 2006; 163: 2157–63.
- Cootes TF, Edwards GJ, Taylor CJ. Active appearance models. *IEEE Trans Pattern Anal Mach Intell* 2001; 23: 681–5.
- Courchesne E, Mouton PR, Calhoun ME, Semendeferi K, Ahrens-Barbeau C, Hallett MJ, et al. Neuron number and size in prefrontal cortex of children with autism. *JAMA* 2011; 306: 2001–10.
- Cowan WM, Fawcett JW, O'Leary DD, Stanfield BB. Regressive events in neurogenesis. *Science* 1984; 225: 1258–65.
- Deoni SCL, Dean DC, O'Muircheartaigh J, Dirks H, Jerskey BA. Investigating white matter development in infancy and early childhood using myelin water fraction and relaxation time mapping. *Neuroimage* 2012; 63: 1038–53.
- Dinstein I, Pierce K, Eyley L, Solso S, Malach R, Behrmann M, et al. Disrupted neural synchronization in toddlers with autism. *Neuron* 2011; 70: 1218–25.
- Egaas B, Courchesne E, Saitoh O. Reduced size of corpus callosum in autism. *Arch Neurol* 1995; 52: 794–801.
- Elison JT, Paterson SJ, Wolff JJ, Reznick JS, Sasson NJ, Gu H, et al. White matter microstructure and atypical visual orienting in 7-month-olds at risk for autism. *Am J Psychiatry* 2013; 170: 899–908.
- Frazier TW, Hardan AY. A meta-analysis of the corpus callosum in autism. *Biol Psychiatry* 2009; 66: 935–41.
- Frazier TW, Keshavan MS, Minshew NJ, Hardan AY. A two-year longitudinal MRI study of the corpus callosum in autism. *J Autism Dev Disord* 2012; 42: 2312–22.
- Freitag CM, Luders E, Hulst HE, Narr KL, Thompson PM, Toga AW, et al. Total brain volume and corpus callosum size in medication-naïve adolescents and young adults with autism spectrum disorder. *Biol Psychiatry* 2009; 66: 316–19.
- Giedd JN, Blumenthal J, Jeffries NO, Rajapakse JC, Vaituzis AC, Liu H, et al. Development of the human corpus callosum during childhood and adolescence: a longitudinal MRI study. *Prog Neuropsychopharmacol Biol Psychiatry* 1999; 23: 571–88.
- Giedd JN, Castellanos FX, Casey BJ, Kozuch P, King AC, Hamburger SD, et al. Quantitative morphology of the corpus callosum in attention deficit hyperactivity disorder. *Am J Psychiatry* 1994; 151: 665–9.
- Gilmore JH, Shi F, Woolson SL, Knickmeyer RC, Short SJ, Lin W, et al. Longitudinal development of cortical and subcortical gray matter from birth to 2 years. *Cereb Cortex* 2012; 22: 2478–85.
- Goodlett CB, Fletcher PT, Gilmore JH, Gerig G. Group analysis of DTI fiber tract statistics with application to neurodevelopment. *Neuroimage* 2009; 45: S133–42.
- Gotham K, Pickles A, Lord C. Standardizing ADOS scores for a measure of severity in autism spectrum disorders. *J Autism Dev Disord* 2009; 39: 693–705.
- Gottesman II, Gould TD. The endophenotype concept in psychiatry: etymology and strategic intentions. *Am J Psychiatry* 2003; 160: 636–45.
- Gouttard S, Styner M, Prastawa M, Piven J, Gerig G. Assessment of reliability of multi-site neuroimaging via traveling phantom study. *Med Image Comput Assist Interv* 2008; 11: 263–70.
- Gozzi M, Nielson DM, Lenroot RK, Ostuni JL, Luckenbaugh DA, Thurm AE, et al. A magnetization transfer imaging study of corpus callosum myelination in young children with autism. *Biol Psychiatry* 2012; 72: 215–20.
- Hardan AY, Pabalan M, Gupta N, Bansal R, Melhem NM, Fedorov S, et al. Corpus callosum volume in children with autism. *Psychiatry Res* 2009; 174: 57–61.
- Hazlett HC, Poe MD, Gerig G, Styner M, Chappell C, Smith RG, et al. Early brain overgrowth in autism associated with an increase in cortical surface area before age 2 years. *Arch Gen Psychiatry* 2011; 68: 467–76.
- Hofer S, Frahm J. Topography of the human corpus callosum revisited—comprehensive fiber tractography using diffusion tensor magnetic resonance imaging. *Neuroimage* 2006; 32: 989–94.
- Iacono WG, Malone SM. Developmental Endophenotypes: indexing genetic risk for substance abuse with the P300 brain event-related potential. *Child Dev Perspect* 2011; 5: 239–47.
- Just MA, Cherkassky VL, Keller TA, Kana RK, Minshew NJ. Functional and anatomical cortical underconnectivity in autism:

- evidence from an fMRI study of an executive function task and corpus callosum morphometry. *Cereb Cortex* 2007; 17: 951–61.
- Kass M, Witkin A, Terzopoulos D. Snakes: active contour models. *Int J Comp Vision* 1988; 1: 321–31.
- Keary CJ, Minschew NJ, Bansal R, Goradia D, Fedorov S, Keshavan MS, et al. Corpus callosum volume and neurocognition in autism. *J Autism Dev Disord* 2009; 39: 834–41.
- Khan S, Gramfort A, Shetty NR, Kitzbichler MG, Ganesan S, Moran JM, et al. Local and long-range functional connectivity is reduced in concert in autism spectrum disorders. *Proc Natl Acad Sci USA* 2013; 110: 3107–12.
- Klawiter EC, Schmidt RE, Trinkaus K, Liang H-F, Budde MD, Naismith RT, et al. Radial diffusivity predicts demyelination in ex vivo multiple sclerosis spinal cords. *Neuroimage* 2011; 55: 1454–60.
- Kumar A, Sundaram SK, Sivaswamy L, Behen ME, Makki MI, Ager J, et al. Alterations in frontal lobe tracts and corpus callosum in young children with autism spectrum disorder. *Cereb Cortex* 2010; 20: 2103–13.
- LaMantia AS, Rakic P. Axon overproduction and elimination in the corpus callosum of the developing rhesus monkey. *J Neurosci* 1990; 10: 2156–75.
- Langen M, Durston S, Kas MJH, van Engeland H, Staal WG. The neurobiology of repetitive behavior: ... and men. *Neurosci Biobehav Rev* 2011; 35: 356–65.
- Lefebvre A, Beggiano A, Bourgeron T, Toro R. Neuroanatomical diversity of corpus callosum and brain volume in autism: meta-analysis, analysis of the Autism Brain Imaging Data Exchange project, and simulation. *Biol Psychiatry* 2015. Advance Access published on February 17, 2015, doi: 10.1016/j.biopsych.2015.02.010.
- Lenroot RK, Gogtay N, Greenstein DK, Wells EM, Wallace GL, Clasen LS, et al. Sexual dimorphism of brain developmental trajectories during childhood and adolescence. *Neuroimage* 2007; 36: 1065–73.
- Lewis JD, Elman JL. Growth-related neural reorganization and the autism phenotype: a test of the hypothesis that altered brain growth leads to altered connectivity. *Dev. Sci* 2008; 11: 135–55.
- Lewis JD, Evans AC, Pruett JR, Botteron K, Zwaigenbaum L, Estes A, et al. Network inefficiencies in autism spectrum disorder at 24 months. *Transl Psychiatry* 2014; 4: e388.
- Lewis JD, Theilmann RJ, Fonov V, Bellec P, Lincoln A, Evans AC, et al. Callosal fiber length and interhemispheric connectivity in adults with autism: brain overgrowth and underconnectivity. *Hum Brain Mapp* 2013; 34: 1685–95.
- Liu Z, Wang Y, Gerig G, Gouttard S, Tao R, Fletcher T, et al. Quality control of diffusion weighted images. *Proc Soc Photo Opt Instrum Eng* 2010; 7628.
- Lord C, Risi S, Lambrecht L, Cook EH, Leventhal BL, DiLavore PC, et al. The autism diagnostic observation schedule-generic: a standard measure of social and communication deficits associated with the spectrum of autism. *J Autism Dev Disord* 2000; 30: 205–23.
- Lord C, Rutter M, Couteur A. Autism Diagnostic Interview-Revised: a revised version of a diagnostic interview for caregivers of individuals with possible pervasive developmental disorders. *J Autism Dev Disord* 1994; 24: 659–85.
- Low LK, Cheng H-J. Axon pruning: an essential step underlying the developmental plasticity of neuronal connections. *Philos Trans R Soc Lond B Biol Sci* 2006; 361: 1531–44.
- Manes F, Piven J, Vrancic D, Nanclares V, Plebst C, Starkstein SE. An MRI study of the corpus callosum and cerebellum in mentally retarded autistic individuals. *J Neuropsychiatry Clin Neurosci* 1999; 11: 470–4.
- Markham JA, Herting MM, Luszpak AE, Juraska JM, Greenough WT. Myelination of the corpus callosum in male and female rats following complex environment housing during adulthood. *Brain Res* 2009; 1288: 9–17.
- Mori S, Zhang J. Principles of diffusion tensor imaging and its applications to basic neuroscience research. *Neuron* 2006; 51: 527–39.
- Mullen EM. Mullen scales of early learning. Circle Pines, MN: AGS Publishing; 1995.
- Nair A, Treiber JM, Shukla DK, Shih P, Müller R-A. Impaired thalamocortical connectivity in autism spectrum disorder: a study of functional and anatomical connectivity. *Brain* 2013; 136: 1942–55.
- Oguz I, Farzinfar M, Matsui J, Budin F, Liu Z, Gerig G, et al. DTIPrep: quality control of diffusion-weighted images. *Front Neuroinform* 2014; 8: 4.
- Paus T. Growth of white matter in the adolescent brain: myelin or axon? *Brain Cogn* 2010; 72: 26–35.
- Paus T, Toro R. Could sex differences in white matter be explained by g ratio? *Front Neuroanat* 2009; 3: 14.
- Perrin JS, Leonard G, Perron M, Pike GB, Pitiot A, Richer L, et al. Sex differences in the growth of white matter during adolescence. *Neuroimage* 2009; 45: 1055–66.
- Piven J, Arndt S, Bailey J, Haverkamp S, Andreasen NC, Palmer P. An MRI study of brain size in autism. *Am J Psychiatry* 1995; 152: 1145–9.
- Piven J, Bailey J, Ranson BJ, Arndt S. An MRI study of the corpus callosum in autism. *Am J Psychiatry* 1997; 154: 1051–6.
- Prigge MBD, Lange N, Bigler ED, Merkle TL, Neeley ES, Abildskov TJ, et al. Corpus callosum area in children and adults with autism. *Res Autism Spectr Disord* 2013; 7: 221–34.
- Redcay E, Courchesne E. When is the brain enlarged in autism? A meta-analysis of all brain size reports. *Biol Psychiatry* 2005; 58: 1–9.
- Rutter M, Bailey A, Lord C, Berument S. Social communication questionnaire. Los Angeles, CA: Western Psychological Services; 2003.
- Sadeghi N, Prastawa M, Fletcher PT, Wolff J, Gilmore JH, Gerig G. Regional characterization of longitudinal DT-MRI to study white matter maturation of the early developing brain. *Neuroimage* 2013; 68: 236–47.
- Schipul SE, Williams DL, Keller TA, Minschew NJ, Just MA. Distinctive neural processes during learning in autism. *Cereb Cortex* 2012; 22: 937–50.
- Schumann CM, Bloss CS, Barnes CC, Wideman GM, Carper RA, Akshoomoff N, et al. Longitudinal magnetic resonance imaging study of cortical development through early childhood in autism. *J Neurosci* 2010; 30: 4419–27.
- Shen MD, Nordahl CW, Young GS, Wootton-Gorges SL, Lee A, Liston SE, et al. Early brain enlargement and elevated extra-axial fluid in infants who develop autism spectrum disorder. *Brain* 2013; 136: 2825–35.
- Shukla DK, Keehn B, Lincoln AJ, Müller R-A. White matter compromise of callosal and subcortical fiber tracts in children with autism spectrum disorder: a diffusion tensor imaging study. *J Am Acad Child Adolesc Psychiatry* 2010; 49: 1269–78, 1278.e1–2.
- Sparks BF, Friedman SD, Shaw DW, Aylward EH, Echelard D, Artru AA, et al. Brain structural abnormalities in young children with autism spectrum disorder. *Neurology* 2002; 59: 184–92.
- Styner M, Gerig G, Lieberman J, Jones D, Weinberger D. Statistical shape analysis of neuroanatomical structures based on medial models. *Med Image Anal* 2003; 7: 207–20.
- Sun H, Yushkevich PA, Zhang H, Cook PA, Duda JT, Simon TJ, et al. Shape-based normalization of the corpus callosum for DTI connectivity analysis. *IEEE Trans Med Imaging* 2007; 26: 1166–78.
- Székel G, Kelemen A, Brechbühler C, Gerig G. Segmentation of 2-D and 3-D objects from MRI volume data using constrained elastic deformations of flexible Fourier contour and surface models. *Med Image Anal* 1996; 1: 19–34.
- Uddin LQ, Supekar K, Menon V. Reconceptualizing functional brain connectivity in autism from a developmental perspective. *Front Hum Neurosci* 2013; 7: 458.

- Vachet C, Yvernault B, Bhatt K, Smith RG, Gerig G, Hazlett HC, Styner M. Automatic corpus callosum segmentation using a deformable active Fourier contour model. *Proc Soc Photo Opt Instrum Eng* 2012; 23: 8317.
- Verde AR, Budin F, Berger J-B, Gupta A, Farzinfar M, Kaiser A, et al. UNC-Utah NA-MIC framework for DTI fiber tract analysis. *Front Neuroinform* 2014; 7: 51.
- Vidal CN, Nicolson R, DeVito TJ, Hayashi KM, Geaga JA, Drost DJ, et al. Mapping corpus callosum deficits in autism: an index of aberrant cortical connectivity. *Biol Psychiatry* 2006; 60: 218–25.
- Waiter GD, Williams JHG, Murray AD, Gilchrist A, Perrett DI, Whiten A. Structural white matter deficits in high-functioning individuals with autistic spectrum disorder: a voxel-based investigation. *Neuroimage* 2005; 24: 455–61.
- Witelson SF. Hand and sex differences in the isthmus and genu of the human corpus callosum: a postmortem morphological study. *Brain* 1989; 112: 799–835.
- Wolff JJ, Botteron KN, Dager SR, Elison JT, Estes AM, Gu H, et al. Longitudinal patterns of repetitive behavior in toddlers with autism. *J Child Psychol Psychiatry* 2014; 55: 945–53.
- Wolff JJ, Gu H, Gerig G, Elison JT, Styner M, Gouttard S, et al. Differences in white matter fiber tract development present from 6 to 24 months in infants with autism. *Am J Psychiatry* 2012; 169: 589–600.
- Workman AD, Charvet CJ, Clancy B, Darlington RB, Finlay BL. Modeling transformations of neurodevelopmental sequences across mammalian species. *J Neurosci* 2013; 33: 7368–83.
- Zielinski BA, Prigge MBD, Nielsen JA, Froehlich AL, Abildskov TJ, Anderson JS, et al. Longitudinal changes in cortical thickness in autism and typical development. *Brain* 2014; 137: 1799–812.
- Zikopoulos B, Barbas H. Changes in prefrontal axons may disrupt the network in autism. *J Neurosci* 2010; 30: 14595–609.

Appendix 1

The Infant Brain Imaging Study (IBIS) Network is an NIH funded Autism Centre of Excellence project and consists of a consortium of eight universities in the U.S. and Canada. Clinical Sites: University of North Carolina: J. Piven (IBIS Network PI), H.C. Hazlett, C. Chappell; University of Washington: S. Dager, A. Estes, D. Shaw; Washington University: K. Botteron, R. McKinstry, J. Constantino, J. Pruett; Children's Hospital of Philadelphia: R. Schultz, S. Paterson; University of Alberta: L. Zwaigenbaum; University of Minnesota: J. Elison; Data Coordinating Centre: Montreal Neurological Institute: A.C. Evans, D.L. Collins, G.B. Pike, V. Fonov, P. Kostopoulos; S. Das; Image Processing Core: University of Utah: G. Gerig; University of North Carolina: M. Styner; Statistical Analysis Core: University of North Carolina: H. Gu.